At the time of issue this report has not been published. Any author desiring to quote this paper should refer to it as "A paper of the Meteorological Research Committee (London).
M.R.P. No.896 by Mr. J.S. Sawyer
A copy is available in the Library of the Meteorological Office."

M.R.P. 896
S.C.II/183
31st December, 1954.

AIR MINISTRY
METEOROLOGICAL RESEARCH COMMITTEE

Some characteristics of fronts and their relation to frontogenesis

by
J.S. Sawyer (Meteorological Office)

1. Introduction

Although the Norwegian system of frontal analysis has been generally accepted by weather forecasters since the 1920's, no satisfactory explanation has been given for the "up-sliding" motion of the warm air to which is attributed the characteristic frontal cloud and rain. Simple dynamical theory shows that a sloping discontinuity between two air-masses with different density and velocity can exist without vertical movement of either air-mass, and in order to explain the associated field of vertical motion it is necessary to invoke secondary effects not specifically associated with the existence of the sloping frontal zone. J.Bjerknes (1924) relates the vertical velocities to the horizontal accelerations of the air parallel to the front and the same effect is considered in the somewhat more detailed mathematical analysis of Sawyer (1952a). Surface friction has been considered by Brunt (1941) and found inadequate to account for more than a fraction of the observed vertical motion, and turbulent mixing in the free atmosphere has been considered by Raethjen (1953). None of these explanations is entirely satisfactory as a fundamental explanation of the association between fronts and rain, because none appears to apply to all active fronts. The processes considered may however be important in modifying the structure of individual fronts.

The purpose of the present paper is to suggest that a front should not be considered so much as a stable area of strong temperature contrast between two air masses, but as an area into which active confluence of air currents of different temperature is taking place. There are several processes, friction, turbulence and vertical movements, which might be expected to destroy the sharp temperature contrast of a front within a day or so of its formation, so it would not be surprising if clearly defined fronts were found only where active frontogenesis is in progress. Some synoptic evidence for this point of view will be presented, and it will also be demonstrated that the frontogenetic process is necessarily accompanied by a vertical circulation system which can explain several characteristic features of the structure of fronts.

There is one essential difficulty which will beset any attempt to attribute the existence of fronts to any particular physical or dynamical process, namely the uncertainty as to what constitutes a front. The weather maps drawn independently by two synoptic analysts have only to be compared to show that the placing of fronts on the synoptic charts is not an objective process. With such a large uncertainty as to whether a front does or does not exist, one cannot expect to find any exact correspondence between the existence of a front on the synoptic chart and some specific physical process. On the other hand there are certain fronts which no experienced analyst would question, and there is no doubt that a systematic organisation of wind, pressure, cloud and rain occurs with them. The method adopted in the present paper is to study primarily fronts which are active and reasonably well defined and to present (in several different ways) the evidence that frontogenesis was in progress. Although a unique relationship is neither found nor expected between

/the

the existence of a front and the process of frontogenetic confluence of the horizontal flow, the evidence suggests a close association, and is believed to be adequate to show that the existence of recognisable frontal characteristics may owe much to the dynamics and kinematics of the process of frontogenesis.

2. The trajectories of air near fronts

Trajectories have been drawn of the air found in the vicinity of twenty active fronts, and serve to illustrate that the air parcels on opposite sides of the frontal zone usually have distinctly different tracks over the preceding 24 hr. The fronts, ten warm fronts and ten cold fronts, were chosen to cover a variety of synoptic situations, the sole restriction on the choice being that the front should be active and its identification reasonably unambiguous.

Air trajectories were drawn to terminate at a set of points in a vertical plane perpendicular to the front, spaced at about 100 mi intervals across the front. The trajectories were drawn separately for the 2,000 ft, 700 mb, 500 mb and 300 mb levels and covered a 24-hr period; they were based on the horizontal movement of air at these levels as deduced from appropriate measurements of geostrophic wind, supplemented by such direct wind observations as were available. Temperatures at points along the trajectories were estimated where possible by interpolation between soundings adjacent to the track, and these temperatures have been used to make some estimate of vertical motion.

Although there is evidence that vertical motion was present, such vertical movement was not sufficient to make the trajectories based on winds at one level seriously unrepresentative of the true movement of the air, and in view of the uncertainties in any drawing of air trajectories, no correction was attempted for vertical displacements.

Inspection of the air trajectories shows that air from widely different regions is frequently drawn into frontal regions. Although it is difficult in some individual cases to decide whether such a "confluent" process is present, in many cases the existence of such confluence is undeniable. A subjective assessment of the presence or absence of a marked difference in the trajectories of air on the warm and cold side of the frontal zone showed that such a difference existed in 19 cases out of 20 at the 2,000 ft level, 14 at 700 mb, 10 at 500 mb and 7 at the 300 mb levels. The single case in which no definite confluence was noted at any level was one in which the rain area was not aligned along the front and the well-defined frontal cloud system was absent.

As a rough measure of the degree of confluence the ratio of the distances between the initial and terminal points of the trajectories was calculated for trajectories terminating at points 200 to 300 mi apart enclosing the frontal zone. The mean values were 2.1, 2.7 and 3.0 for the 2,000 ft, 700 mb and 500 mb levels respectively. Values greater than unity show that the air particles were approaching one another, but some apparent confluence is inevitable from the fact that the trajectories were all drawn to terminate at points near together. As a basis for comparison 20 pairs of trajectories were also drawn to terminate at similarly spaced points in air masses away from fronts. The corresponding mean ratios of the initial and terminal distances between the air parcels namely 1.7, 1.6 and 2.1 for the 2,000 ft, 700 and 500 mb levels are definitely less than the values associated with frontal regions.

The fronts examined covered a wide variety of synoptic situations, and there was little similarity between the trajectories in different cases. It does, however, seem possible to draw a distinction between those cases in which the confluent flow pattern extended through most of the troposphere and those in which it was primarily a feature of the layer up to 700 mb. Typically, the former were associated with a well developed jet stream; in some cases they were associated with an obviously confluent pattern of stream lines at all levels but in other cases the confluence of the stream lines was not obvious

/and

and the confluence of the trajectories owes something to the movement of the stream-line pattern. A case of high-reaching confluence is illustrated by trajectories terminating at 0300 16 Aug. 1949 (Fig.1). A noteworthy feature is the fact that the line separating the two types of trajectories is displaced towards the cold air with increasing height.

An example of a front extending only to mid-troposphere with confluent flow only in the lower troposphere is given by the warm front of 3 May 1948 (Fig.2). No clear-cut confluence is found above the 700 mb level. Such cases are found mainly among fast moving warm fronts which are not clearly defined at high levels and which are not associated with the jet stream in the conventional manner. The rapid changes in the surface pressure field play an important part in bringing together air of widely different origin.

Inspection of the air temperature along the (horizontal) trajectories shows that cooling is frequent on the warm side of the frontal zone and warming on the cold side, indicative of descent of the cold air and ascent of the warm air. Fairly definite evidence of such vertical motion exists for 13 of the 20 fronts examined, in four cases the evidence is inconclusive and in three the vertical motion appears to have been slight. Table I was obtained by classifying the vertical motion of the air parcels according as the trajectory terminated in the warm, transitional or cold air mass. A change of 5°F or more in 12 hr was required before a case was classified as one of warming or cooling. The tendency at the 700 mb and 500 mb levels for cooling along the trajectory in the warm air mass and warming in the cold air mass is apparent. The temperature contrast between the air parcels moving into the frontal zone was reduced in 12 cases out of 14 at the 700 mb and 10 out of 11 at the 500 mb levels; the mean ratio of the final to the initial temperature difference being 0.74 at 700 mb, 0.71 at 500 mb and 0.77 at 300 mb.

Table I - Classification of temperature changes following horizontal air trajectories near frontal zones

Level	Warm Air			Transitional Air			Cold Air		
	Warming	Little change	Cooling	Warming	Little change	Cooling	Warming	Little change	Cooling
				(number of cases)					
700 mb	0	16	5	4	15	5	12	18	1
500 mb	0	27	6	15	2	1	4	3	3
300 mb	8	20	9	3	1	2	0	3	0

These temperature changes are consistent with a vertical air circulation upward in the warm air and downward in the cold air which tends to reduce the temperature contrast across the front; a contrast which is maintained primarily by the confluence of the air flow.

3. The field of frontogenesis in the vicinity of fronts-individual cases

The kinematics of frontogenesis have been considered by a number of writers, in particular by Bergeron (1928) and Petterssen (1935)[*].
It can be shown directly that at any point in a two-dimensional field of flow two adjacent fluid elements will approach or separate at a rate which depends on the orientation of the line joining the fluid elements as well as on the derivatives of the components of velocity u and v. The orientations

/for

Footnote[*] Throughout this paper "frontogenesis" has been taken to mean a condition of increasing horizontal temperature gradient. This is not exactly the same interpretation as that used by Petterssen who requires that a maximum rate of increase of horizontal temperature gradient should occur along a line.

for maximum expansion of the distance between the particles and for maximum contraction are mutually perpendicular; they are the axes of strain in the deformation field. Here they will be referred to as the "axis of dilatation" and "axis of contraction". In large scale meteorological systems of the size of depressions and anticyclones, and even down to the scale of fronts, a first approximation to the flow is given by the geostrophic wind field. Neglecting the variation of the Coriolis parameter with latitude, the geostrophic wind field is non-divergent, and it is readily shown that the rate of separation between two air parcels separated by a small distance S is given by

$$\frac{1}{S}\frac{\partial S}{\partial t} = \frac{1}{2}(A^2 + B^2)^{1/2} \cos 2\phi$$

where ϕ is the angle between the orientation of the line joining the fluid elements and the orientation which gives maximum contraction; following the notation of Petterssen (1953), A and B are defined by

$$A = \frac{\partial u}{\partial x} - \frac{\partial v}{\partial y} \qquad \text{and} \qquad B = \frac{\partial u}{\partial y} + \frac{\partial v}{\partial x}$$

The angle, θ, between the direction for maximum contraction and the x-axis is given by

$$\cot \theta = \frac{A}{B} - \frac{1}{B}(A^2 + B^2)^{1/2}$$

(The positive sign of the square root is to be used in the preceding equations).

If geostrophic flow is assumed, A and B are readily calculated from a contour chart of an appropriate isobaric level. A simple method is to place a transparent scale of the form illustrated in Fig. 3 on the chart, and to evaluate A and B from the relations.

$$A = \frac{1}{a^2 l} g \left(H_D + H_H - (H_F + H_B) \right)$$

$$B = \frac{1}{a^2 l} g \left(H_A + H_E - (H_C + H_G) \right)$$

The symbol H_X indicates the value of the contour height at point X, g is the acceleration due to gravity, l is the Coriolis parameter and a is the radius of the circle on the scale in terms of map distance. If a corresponds to 168 nautical mi the multiplying factor $g/a^2 l$ becomes 1/10 in latitude 50°N. for values of H in units of 100 ft and values of A and B in units hr^{-1}. Such a scale has been used to evaluate A and B in the work which is described below.

It will be seen that the maximum rate of approach of any two adjacent fluid elements is proportional to $(A^2 + B^2)^{1/2}$. Thus this expression gives a measure of the maximum degree of frontogenesis in the given velocity field, and in order to realise this effect the isotherms must be orientated in the direction of the axis of dilatation. For any other orientation the rate of concentration of the temperature gradient is proportional to $(A^2 + B^2)^{1/2} \cos 2\phi$ where ϕ is the angle between the isotherms and the axis of dilatation. The velocity field will thus be frontogenetic or frontolytic according as the isotherms lie within 45° of the axis of dilatation or not.

Several charts have been drawn to show the distribution of the values of $1/2(A^2+B^2)^{1/2}$ and $1/2(A^2+B^2)^{1/2} \cos 2\phi$ in the vicinity of fronts. The charts have been calculated for the 700 mb level because although this level is within the lower troposphere and results may be related to surface fronts, the contour lines as drawn at C.F.O. are not distorted to conform to any conventional idea of the distribution of pressure in the vicinity of fronts.

Most of these charts show areas in which $\frac{1}{2}(A^2+B^2)^{1/2} \cos 2\phi$ has a maximum lying to the cold side of surface fronts. The correspondence is not perfect, but is sufficient to suggest that active frontogenesis is an important feature

of the frontal organisation. An example of such a chart is provided by the cold front of 5 Nov. 1949 (Fig. 4). A well defined maximum of $\frac{1}{2}(A^2+B^2)^{1/2}$ lies parallel to the front and slightly to the cold side; it coincides closely with the position of the front at 700 mb. The axis of dilatation and the directions of the isotherms are nearly parallel in this region and the expression for the frontogenesis $\frac{1}{2}(A^2+B^2)^{1/2}\cos 2\phi$ also has a well defined maximum. The maximum of $\frac{1}{2}(A^2+B^2)^{1/2}$ in the west is less important because of the absence of any substantial thermal gradient, and because such thermal gradient as there is does not closely parallel the axis of dilatation over any significant area.

4. The field of frontogenesis in the vicinity of a series of fronts

In order to obtain some further information about the distribution of the field of frontogenesis in the vicinity of fronts, all of the active and well defined fronts occurring in the vicinity of the British Isles during January 1953 were examined. On each six-hourly chart on which such a front appeared, the values of $\frac{1}{2}(A^2+B^2)^{1/2}$ and $\frac{1}{2}(A^2+B^2)^{1/2}\cos 2\phi$ (in the notation of the preceding section) were calculated for a series of points extending at 200 mi intervals from the position of the surface front towards the cold air. These calculations were carried out separately for the 1,000 mb, 700 mb and 300 mb levels. It was found difficult to analyse the temperature field satisfactorily at 1,000 mb and 300 mb; at the former level the difficulty arose from the unrepresentative nature of surface temperatures and at the latter from the complications introduced by the tropopause. The direction of the 1,000 - 700 mb thickness lines and 500 - 300 mb thickness lines were therefore used to define a direction representative of the run of the isotherms in the lower and upper troposphere for use in determining the angle ϕ .

Histograms showing the frequency of values of $\frac{1}{2}(A^2+B^2)^{1/2}$ and $\frac{1}{2}(A^2+B^2)^{1/2}\cos 2\phi$ in various ranges are displayed in Figs. 5 and 6 for the individual points I, II, III and IV which were chosen to be 0, 200, 400 and 600 mi from the surface front respectively. The mean values are also given. Histograms are also given for the 700 mb level in respect of 22 cases of inactive fronts occurring during the first half of the month.

The important fact demonstrated by these histograms is the tendency for $\frac{1}{2}(A^2+B^2)^{1/2}\cos 2\phi$ to be positive near active fronts at the surface and 700 mb levels. From the frequency distribution the standard error of the mean is estimated to be about $0.06 \times 10^{-1}\,hr^{-1}$, so that it is clear that the mean values of $\frac{1}{2}(A^2+B^2)^{1/2}\cos 2\phi$ are significantly greater than zero for points 0, 200 and 400 mi from an active front at the surface and 0 and 200 mi from an active front at 700 mb. The mean values for inactive fronts are negative at three points and positive at one, but barely exceed twice the estimated standard error. At 300 mb the positive values at points II and III exceed twice the estimated standard error but the negative values at points I and II do not. It may be concluded that there is a definite tendency for the axis of dilatation to lie within 45^0 of the isotherms in an active frontal region, but not in an inactive one. The effect is particularly well-marked at 700 mb at a distance of 200 mi from the surface front where 38 out of the 42 values of $\frac{1}{2}(A^2+B^2)^{1/2}\cos 2\phi$ were positive.

The mean values of $\frac{1}{2}(A^2+B^2)^{1/2}$ do not differ significantly between active and inactive fronts, nor between the individual points at various distances from the front. This suggests that the orientation of the local axis of dilatation with respect to the isotherms is a more important factor in determining the activity of a front than the actual intensity of the deformation field.

The values of $(A^2+B^2)^{1/2}$ are greater for 300 mb than for the lower levels. This is partly an effect of the stronger winds at higher levels but may also arise in part from the greater errors of estimation at these high levels. Vuorela (1953) has pointed out that the neglect of the ageostrophic components of wind leads to an overestimate of the dilatation.

/Included

Included among the fronts of Jan. 1951 was one warm front which moved across the British Isles with very little change of form. It was active in the north and inactive in the south and it was possible to estimate the values of the dilatation on both active and inactive sections over a sequence of five charts at 6-hr intervals. The mean values of $\frac{1}{2}(A^2+B^2)^{1/2}\cos 2\phi$ so obtained are displayed in vertical section in Fig. 7, together with the axis of dilatation of the mean flow at 700 mb at several points placed with respect to the front. The axis of dilatation is seen to closely parallel the isotherms near the active section of the front leading to a well-defined maximum frontogenetic effect about 200 mi ahead of the active part of the front. This is also shown at the surface, but at 500 mb and 300 mb the maximum is split, part being 400-600 mi ahead of the surface front and part vertically above it. The values of the frontogenesis on the inactive section of the front are smaller and no clearly defined pattern is apparent.

5. Theoretical aspects of the role of confluence in fronts

Some idea of the possible role of the confluence process in the dynamics of fronts may be obtained from the consideration of a much simplified case. This is illustrated in Fig. 8 by horizontal and vertical sections. It is clear that a horizontal flow such as illustrated in Fig. 8 (a) would be expected to concentrate the temperature gradient near the central straight stream line. The flow is assumed to have the same general form at all levels, but as approximate geostrophic balance is required, the velocity in the direction of the isotherms will increase with height and the isokinetics will have the general form shown in the vertical cross-section Fig. 8(b).

As the thermal gradient increases the vertical wind shear must also increase if approximate geostrophic flow is maintained. Thus either the high level winds will be accelerated or the low level winds will be retarded and in either case a cross-isobaric flow towards the cold air aloft must be expected relative to the flow at lower levels. This arises from the well known relation between the acceleration of the air and its ageostrophic movement (see Sutcliffe 1938). A vertical circulation of the type indicated in Fig. 8(b) must result because the cross-isobaric flow will be much less at a distance from the axis of confluence than in the frontal zone because the thermal gradients are much less at a distance.

The preceding simple argument may be made the basis of mathematical calculation in order to estimate the numerical values of the vertical and cross-isobar movements. It is then possible to make some allowance for the effect of the vertical air-movement on the temperature field. Geostrophic flow will be assumed to be adequate to represent the flow parallel to the isotherms, but no such assumption will be made regarding the flow in the perpendicular direction.

We take the x axis in the direction of the isotherms in Fig. 8(a) which are assumed straight and parallel at all levels, and we use isobaric coordinates. The horizontal components of velocity are then u and v, and the vertical motion is described by $w \equiv dp/dt$. We shall assume that the large-scale field of confluence imposes an extension of fluid elements in the x-direction such that $\partial u/\partial x = F$ and that F is the same everywhere.

The equation of continuity then imposes the following condition on motion in the y, z plane.

$$\partial v/\partial y + \partial w/\partial p = -F \qquad (1)$$

In order to simplify the mathematics we shall treat the atmosphere as an incompressible frictionless fluid of specific volume α . The variations of α from place to place then represent the temperature gradients in the atmosphere. It seems likely that the essential characteristics of the motion will not be affected by this neglect of compressibility except in so far as the vertical variation of height as a function of pressure is changed.

/The

The assumption that geostrophic flow is an adequate representation of the motion in the x -direction implies that

$$lu = -g\frac{\partial h}{\partial y} \qquad (2)$$

where h is the height of an isobaric surface.

If we write u_g and v_g for the components of the geostrophic wind then

$$\frac{\partial u_g}{\partial x} = -\frac{\partial v_g}{\partial y} = \frac{-g}{l}\frac{\partial^2 h}{\partial x \partial y}$$

As we have assumed that $\partial u/\partial x = F$ and that the motion in the x -direction is adequately treated as geostrophic, it follows that $\partial v_g/\partial y = -F$ and without further loss of generality we can write $v_g = -Fy$. The x-component of the equations of motion can, therefore, be written,

$$\frac{\partial u}{\partial t} + u\frac{\partial u}{\partial x} + v\frac{\partial u}{\partial y} + w\frac{\partial u}{\partial p} = l(v + Fy) \qquad (3)$$

The hydrostatic equation gives

$$g\frac{\partial h}{\partial p} = -\alpha \qquad (4)$$

and combining with Eq. (2) we obtain the thermal wind equation $l\partial u/\partial p = \partial\alpha/\partial y$

The conservation of density requires

$$\frac{\partial \alpha}{\partial t} + v\frac{\partial \alpha}{\partial y} + w\frac{\partial \alpha}{\partial p} = 0 \qquad (5)$$

By operating on Eq. (3) with $l\,\partial/\partial p$ and on Eq. (5) by $\partial/\partial y$, subtracting and substituting from Eqs. (2) and (4), the following equation is obtained

$$l\frac{\partial v}{\partial p}\frac{\partial u}{\partial y} + l\frac{\partial w}{\partial p}\frac{\partial u}{\partial p} - \frac{\partial v}{\partial y}\frac{\partial \alpha}{\partial y} - \frac{\partial w}{\partial y}\frac{\partial \alpha}{\partial p} = l^2\frac{\partial v}{\partial p} - l\frac{\partial u}{\partial p}\frac{\partial u}{\partial x} - lu\frac{\partial^2 u}{\partial x \partial p} \qquad (6)$$

In view of the equation of continuity (1), the velocities v and w in the y,p - plane may be expressed in terms of a form of stream function by relations

$$v = \frac{\partial \theta}{\partial p} - Fy \qquad w = -\frac{\partial \theta}{\partial y} \qquad (7)$$

Substitution from (7) in Eq. (6) together with the condition $\frac{\partial u}{\partial x} = F$ then gives

$$l\left(l - \frac{\partial u}{\partial y}\right)\frac{\partial^2 \theta}{\partial p^2} + 2\frac{\partial \alpha}{\partial y}\frac{\partial^2 \theta}{\partial p \partial y} - \frac{\partial \alpha}{\partial p}\frac{\partial^2 \theta}{\partial y^2} = 2F\frac{\partial \alpha}{\partial y} \qquad (8)$$

If u and α are known functions of y and p this is a second order partial differential equation for θ which may be solved numerically given suitable boundary conditions. Such solutions have been obtained for selected density and velocity distributions and show the vertical circulation which should be expected to accompany them. Substitution of the calculated velocities into Eq. (5) gives $\partial\alpha/\partial t$ and shows how the density distribution should respond to the confluent wind field.

/It

It is natural to solve Eq. (8) over an area of the y,p plane bounded by two pressure surfaces $p = p_1$, and $p = p_2$ and two verticals $y = y_1$, and $y = y_2$ chosen to be well outside the baroclinic zone. We can assume that $w = 0$ for $p = p_1$, and $p = p_2$ and that the motion across the planes $y = y_1$, and $y = y_2$ is purely that resulting from the geostrophic confluent wind field which is the basis of the frontogenesis. The boundary conditions then become $\theta = 0$ at all boundary points.

For the purposes of numerical solution it is desirable to use units of length and pressure which permit the grid length used in solving the equation to be one unit and which give values of the coefficients of the order of magnitude of unity. It is also convenient to replace the variables y, p etc. by non-dimensional variables $y' = y/y_o$ where y_o is the selected unit of length etc.

The units which have been found convenient are

$$y_o = 50 \text{ nautical mi}, \quad p_o = 133 \text{ mb}, \quad t_o = 10 \text{ hr}$$

and $\alpha_o = 10/1.28$ gm cm^{-3} (i.e. roughly one hundredth of the normal specific volume of air near the ground).

With these units Eq. (8) becomes (in latitude 50°N.)

$$\left(1 - \frac{1}{4}\frac{\partial u'}{\partial y'}\right)\frac{\partial^2\theta'}{\partial p'^2} + 2\frac{\partial\alpha'}{\partial y'}\frac{\partial^2\theta'}{\partial p'\partial y'} - \frac{\partial\alpha'}{\partial p'}\frac{\partial^2\theta'}{\partial y'^2} = 2F'\frac{\partial\alpha'}{\partial y'} \qquad (9)$$

It is useful to recall that $\frac{\partial\alpha'}{\partial y'} = 1$ corresponds to a density gradient of 1 part in 100 in 50 nautical mi or approximately 6°C (11°F) in 100 mi. Also $\frac{\partial\alpha'}{\partial p'} = 1$ corresponds to a density gradient of 1 part in 100 in 133 mb. A corresponding lapse rate in the real atmosphere will depart by 3°C in 133 mb or roughly 2.5° C/Km from the appropriate dry or saturated adiabatic lapse rate. A reasonable representative value of $\frac{\partial\alpha'}{\partial p'}$ for an atmosphere without saturation would therefore be about 2. When saturation occurs near fronts the lapse rate in the warm air is frequently close to the moist-adiabatic and corresponding values of $\frac{\partial\alpha'}{\partial p'}$ may be less than $\frac{1}{2}$.

Eq. (8) is of the elliptic, parabolic or hyperbolic type according as the following expression is greater, equal to or less than zero.

$$\left(1 - \frac{\partial u}{\partial y}\right)\left(-\frac{\partial\alpha}{\partial p}\right) - \left(\frac{\partial\alpha}{\partial y}\right)^2$$

The condition that Eq. (8) should be elliptic is easily shown to be equivalent to the condition obtained by Solberg (1936) for dynamic stability of a steady baroclinic current. This is often quoted in the form

$$1 - \left(\frac{\partial u}{\partial y}\right)_\alpha > 0 \qquad (10)$$

where $\left(\frac{\partial u}{\partial y}\right)_\alpha$ indicates differentiation along an isentropic surface.

If Eq. (8) is elliptic, that is if the motion is dynamically stable, a unique solution for θ can be determined if θ is known round the boundary.

If Eq. (8) is hyperbolic, that is if the motion is dynamically unstable, a unique solution is not always determined by the boundary values of θ, and it is possible to have non-zero solutions for θ without frontogenesis ($F = 0$). These correspond to the unstable circulations envisaged by perturbation theory.

/Condensation

Condensation processes may be important in determining the dynamical stability of the motion. This can be demonstrated by introducing a modification into the incompressible fluid model to correspond to the effect on the air density of the release of latent heat. We assume that instead of being governed by the requirement of constancy following the fluid motion, namely $\frac{d\alpha}{dt} = 0$, α satisfies the relation

$$\frac{d\alpha}{dt} = -\gamma w \qquad (11)$$

where $\gamma \geq 0$ in non-saturated areas and $\gamma > 0$ in areas corresponding to cloud. Eq. (8) then becomes

$$l(1 - \partial u/\partial y)\frac{\partial^2\theta}{\partial p^2} + 2\frac{\partial\alpha}{\partial y}\frac{\partial^2\theta}{\partial p \partial y} - (\partial\alpha/\partial p + \gamma)\frac{\partial^2\theta}{\partial y^2} = 2F\frac{\partial\alpha}{\partial y} \qquad (12)$$

and since the condition for dynamical instability involves γ , dynamical instability can arise in a previously stable situation solely on account of the occurrence of saturation.

Dynamic instability is unlikely to be a persistent feature of meteorological systems because the effect of friction operating within the unstable circulations would be to return the system to neutral stability. However the case of neutral dynamic stability may be a significant one and one case with neutral stability in part of the field has been included among those studied numerically.

Examination of a number of cross-sections through fronts confirms that the condition for dynamical instability is rarely, if ever, satisfied except in very limited regions, but the condition of neutral stability is frequently approached and probably reached on the upper troposphere on the warm side of the jet stream and (under saturated conditions) within the cloud mass that lies below this region.

In order to study the nature of the vertical circulation Eq. (9) has been solved for θ' by relaxation methods under a number of different conditions. The results are outlined in the following paragraphs and illustrated in Figs. 9 to 12. The solution has been carried out over a grid of points separated by unit distances of y' and p' . The grid extended from $p' = 0$ to $p' = 6$ (say from 200 to 1000 mb) and sufficiently far in the y'-direction to ensure that the solution in the central area was not materially affected by the lateral boundary conditions. In Figs. 9 to 12 the results are displayed in terms of meteorological units with a logarithmic pressure scale, in order to facilitate comparison with the atmosphere. The fields of vertical and horizontal motion normal to the front are shown together with the resulting rate of change of the field of specific volume. The assumed field of specific volume α is also shown, and these isopleths can be regarded as equivalent to isopleths of potential temperature in the atmosphere.

In all cases the value of F' has been taken to be unity corresponding to $\frac{\partial u}{\partial y} = 0.1\ hr^{-1}$ i.e. an extension of the fluid elements of ten per cent per hour in the x- direction.

Case I (Fig. 9)

The distribution of α' was assumed to be given by

$$\alpha' = -\left(\tan^{-1}\frac{y'}{2} + 2p'\right)$$

This corresponds to a vertical frontal zone with a horizontal density gradient equivalent to an air mass difference of temperature of 5°C, of which half is concentrated in a distance of 100 mi. The vertical density gradient is appropriate to a lapse rate of about $\frac{3}{4}$ of the dry adiabatic in dry air. The boundary conditions assume no motion across the isobaric surfaces at 1000 mb and 200 mb and no ageostrophic motion at 900 mi from the front.

/The

The field of vertical motion has maxima of about 3.4 mb/hr situated about 100 mi from the axis of main temperature contrast; the warm air ascends and the cold air descends. There is a slight asymmetry in the field of vertical motion with the zero isopleth inclined upward towards the warm air. Cross-isobar flow has a maximum of about 5 kt at the top and bottom of the layer considered - it is directed towards the warm air near the ground and towards the cold air aloft. The concentration of the density gradient by the confluent wind field is largely confined to the top and bottom quarter of the layer - density changes in the middle of the layer are small, the effect of the horizontal confluence being largely balanced by the vertical movements.

Case II

The distribution of α' was assumed to be

$$\alpha' = -(\tan^{-1} y'/2 + 2p')$$

This case is similar to the preceding one except that the total density contrast across the front is twice as great but is assumed spread over twice the distance (i.e. total contrast equivalent to 10°C of which half is concentrated in a distance of 200 mi). The computed patterns of vertical and horizontal motion are similar - the maxima of vertical movements being about 4.6 mb/hr and about 150 mi from the maximum temperature gradient. Maximum horizontal ageostrophic winds are about 7 kt.

Case III

Case III shows the pattern of vertical and horizontal motion that would be expected to accompany confluence at a sloping frontal zone. The distribution of specific volume is taken to be

$$\alpha' = -\tan^{-1}(y'/2 + p' - 3) - 2p'$$

and corresponds to the same horizontal temperature contrast as in case II but the frontal transition zone has a slope of about 1 in 100. The patterns of vertical and horizontal motion are similar to case II; they are inclined in the direction of the front but rather less steeply; the vertical velocities are somewhat lower than for a vertical frontal zone, but spread over a larger area. The rate of density change is dominated by the tendency of the confluent winds to increase the slope of the front, but again there is little density change in the middle of the troposphere.

Case IV (Fig. 11)

This is similar to case II but some allowance for the effect of condensation has been made. It has been arbitrarily assumed that the ascending air is saturated in the shaded area and that the vertical stability in this area has thereby been reduced to $\frac{1}{4}$ of its value elsewhere. The general patterns of vertical and horizontal motion are not greatly affected by the change in the stability although the upward velocity in the less stable area is increased to a maximum of 5.6 mb/hr. The change in the rate of density change is however more striking - the rate of warming in mid-troposphere in the "cloudy" area is twice what it was in case II and a notable tendency to increase in thermal gradient is shown along the cold side of the "cloud".

Case V

Some indication of the effect of the stratosphere has been obtained by solving Eq. (9) over a grid which contained an additional row of points along which it was assumed that the density gradient was the reverse of that at the remaining points. The additional row represented the stratosphere, and the vertical stability was taken to be twice as great ($\partial\alpha'/\partial p' = -4$) as at the remaining points which represented the troposphere.

/The

The grid was too coarse to hope that any detailed structure will be adequately portrayed. However it is probably significant that the vertical and horizontal movements in the troposphere are very little affected by the addition of the stratosphere. Slight upward motion is found in the stratosphere above the frontal zone and a small area of weak downward motion is computed about 100 mi towards the warm air mass; at greater distances from the front the circulation in the stratosphere is computed to be in the same sense as in the troposphere but vertical currents are less than 1/5 of their magnitude in the troposphere.

Case VI (Fig. 12)

As indicated in previous paragraphs the character of the solution of Eq. (9) is likely to be considerably affected if the thermal gradient becomes so great, or the vertical stability becomes so small, that the condition for dynamical instability (10) is approached. It was therefore considered desirable to carry out the solution of Eq. (9) for a case in which the condition for neutral dynamical stability was satisfied through a large part of the warm air mass. The example and solution are illustrated in Fig. 12.

The distribution of specific volume which was assumed corresponded to a sloping baroclinic zone with a slope of 133 mb in 50 mi, and to a total temperature contrast of about 15°C of which half is concentrated in a distance of 100 mi. The form used for α' was

$$\alpha' = -\frac{3}{2}\tan^{-1}(y' + p') - 2p'$$

The region above midpoint of the frontal zone was assumed to be saturated with water vapour and the value of γ in Eq. (11) was taken to be 2. This implies neutral vertical stability of the warm air at a distance from the front, but slight vertical stability in the vicinity of the front. The dynamical stability of the system depends also on the horizontal wind shear, and it is possible to specify the distribution of the component of velocity in such a way as to give neutral dynamical stability in the warm air above the frontal surface but not elsewhere.

The choice of u' to effect this was

$$u' = F(y') - 6\tan^{-1}(y' + p')$$

where $F(y') = 4y'$ for $-7/2 \leq y' \leq +7/2$

$F(y') = -14$ for $y' \leq -7/2$

$F(y') = +14$ for $y' \geq +7/2$

This distribution of u' is not unrealistic as it implies a cyclonic shear in the vicinity of the front, and an anticyclonic shear in the cold air beneath the frontal zone.

The solution of Eq. (9) for this case is illustrated in Fig. 12. Its detail must not be regarded as of much relevance to the meteorological problem because some features are largely dependent on the somewhat artificial discontinuity between the cloudy and unsaturated air along the thick sloping line. However the following features probably have a more general validity:-

(a) The upward motion is concentrated above the surface position of the front and is of much greater magnitude than computed in the cases in which dynamical instability was not approached (the maximum in Fig. 12 is 29 mb/hr).

(b) Subsidence is found in the cold air. It is spread over a larger area and the speed is less than that of the ascending current.

/(c)

(c) The density gradient between cold and warm air masses is increasing along the boundary of the cloudy region particularly near the ground, although the cold air is being appreciably warmed by subsidence at some distance from the frontal zone.

6. Interpretation of results

In sections 2, 3 and 4 evidence has been collected to show that active confluence is usually in progress in the vicinity of well-defined precipitating fronts. This confluence may extend through the troposphere but on some occasions is confined to the lower half. By considering simple theoretical models it has been shown in section 5 that such a system of confluence in a frontal belt throughout the troposphere requires a vertical circulation in which the warm air mass rises and the cold air mass sinks - a vertical circulation which is confirmed observationally in section 2. It is therefore reasonable to suppose that the characteristic distribution of cloud, rainfall and vertical motion in the vicinity of fronts is derived not solely from the existence of a horizontal temperature gradient but also from the existence of a frontogenetic wind field which tends to concentrate the temperature gradient.

Once the band of cloud and rain is established it will not disperse immediately the frontogenetic wind field is removed and it should not be surprising if fronts are drawn on the weather map without associated frontogenesis. However, such fronts appear to be less active and less well-defined than those associated with marked frontogenesis.

The theoretical discussion of section 5 gives an indication of the magnitude of the horizontal and vertical circulations which may be expected to arise from the proposed mechanism. The rate of rainfall corresponding to any distribution of vertical velocity depends on the temperature and humidity of the air column but for a saturated atmosphere with a wet bulb potential temperature near 50°F the highest values of the vertical velocity computed in any of the theoretical examples of section 5 (with the exception of case VI) correspond to rainfall rates of only 0.5 mm/hr, insufficient to be classed as "moderate" rain. In case VI, in which the density field is such as to give neutral dynamical stability over an extensive cloud mass, the maximum rate of rainfall would be between 2 and 3 mm/hr, a typical rate of steady moderate rainfall.

The various values which have been used for the temperature gradients and rate of frontogenesis etc. in the calculations of section 5 are to some extent arbitrary, but it is unlikely that they seriously underestimate the naturally occurring values. In fact the value of the frontogenesis, F, which has been assumed, namely 0.1 hr^{-1} , is likely to be an overestimate rather than an underestimate of the confluence effect (the mean value of $\frac{1}{2}(A^2+B^2)^{1/2}$ for the 700 mb level in the region of fronts obtained from the analysis of section 4 is only a little over 0.05hr^{-1}). We may therefore conclude that the vertical circulation accompanying frontogenesis is likely to result in only light rainfall unless the distribution of wind and density is such that neutral dynamical stability is approached.

It is not, however, to be expected that all of the vertical motion and rainfall which is observed in the vicinity of fronts owes its origin to characteristics of the front itself. Fronts are usually to be found within regions of cyclonic development where upward motion is to be found as a result of large-scale dynamical factors not directly connected with the front. Indeed recent numerical studies have provided calculated values of the vertical air movement of the correct order of magnitude and distribution to explain the main features of the rainfall distribution without specific consideration of the fronts. Although these calculations may take into account the frontogenetic effect considered in section 5, other dynamical factors also enter into the calculations and are generally of greater importance. It may be remarked that the particular frontogenetic effect, upon which the preceding calculations depend, was omitted from Sutcliffe's treatment of development (Sutcliffe 1947) and

/consequently

consequently was not considered in the calculations of rainfall for the two synoptic situations studied by Sawyer (1952b). Nevertheless the general features of the rainfall distribution were adequately calculated.

It is uncertain whether dynamically unstable conditions occur over sufficiently extensive areas to be important in modifying the vertical circulation, or whether extensive dynamically neutral conditions must be taken into account. However, the occasional occurrence of such conditions together with the existence of superimposed fields of vertical motion associated with the larger scale synoptic systems is probably an adequate explanation of the occurrence of heavy rainfall intensities at some fronts. Making allowance for the occurrence in some cases of near neutral dynamical stability, the theoretical model of section 5 is probably an adequate explanation of the light or moderate rainfall which is more commonly associated with fronts. To resolve the relative importance of the various factors would require a detailed study of individual fronts.

The distribution in Figs. 8 to 12 of $\partial\alpha'/\partial t$, the rate of change of specific volume shows clearly that the rate of intensification of the density gradient is much more rapid near the ground and near the tropopause than it is in mid-troposphere. This conforms with the observed fact that fronts are best defined in the lowest and highest layers of the troposphere. The gradient of $\partial\alpha'/\partial t$ found near the cold boundary of the assumed cloud mass in Figs. 11 and 12 suggests that the condensation process may be an important factor in concentrating the temperature gradient in mid-troposphere near the cold boundary of the cloud.

In Fig. 12 ageostrophic winds of 15 kt are shown blowing across the direction of the front; these values may be rather too large, but values of say 10 kt would imply a difference in the transverse velocity between lower and upper troposphere of 20 kt. Over ten hours such a shear could cause a displacement of the frontal zone in the upper troposphere of 200 mi from its surface position. This transverse circulation may be a significant factor contributing to the slope of a front although it probably is not the only one. The frontogenetic properties of the wind field are not usually as uniform as assumed in the theoretical model and may have a maximum which is displaced towards the cold air at higher levels. This is also suggested by the kinematic analysis of a depression given by Sawyer (1953).

7. Conclusions

The large scale circulation around depressions and anticyclones inevitably contains regions of confluence and when these are associated with a temperature gradient perpendicular to the axis of dilatation frontogenesis results. This frontogenesis leads to a vertical circulation which causes the ascent of the warm air and descent of the cold air and the formation of an inclined frontal zone.

Synoptic evidence suggests that such frontogenesis is in progress in association with most active fronts and it seems likely that they owe their characteristic features to it.

The theoretical discussion which has been given necessarily applies to a very much simplified model. Fronts will usually be found in areas where active cyclogenesis is in progress as a result of dynamical developments on a larger scale so that the characteristic frontal pattern of vertical motion is superimposed upon that resulting from the larger scale cyclogenesis. It is thus not to be expected that all the rainfall found in the vicinity of fronts is to be explained from the frontogenetic process, although the explanation of the characteristic frontal distribution of cloud and rain probably lies therein.

/References

References.

Bergeron, T.	1928	Geofysiske Publikasjoner, Oslo, Vol. 5, No. 6.
Bjerknes, J.	1924	Geofysiske Publikasjoner, Oslo, Vol. 3, No. 6.
Brunt, D.	1941	Physical and Dynamical Meteorology (second edition), p.353.
Petterssen, S.	1935	Geofysiske Publikasjoner, Oslo, Vol. 11, No. 6.
	1953	Tellus, Stockholm, Vol. 5, p. 231.
Raethjen, P.	1953	Dynamik der Zyklonen, Leipzig, pp.164, 165.
Sawyer, J.S.	1952(a)	Quart J. R.Met. Soc., London, Vol. 78, p. 170.
	1952(b)	Quart J. R.Met. Soc., London, Vol. 78, p.231.
	1953	Proceedings Toronto Met.Conference, p. 145.
Solberg, H.	1936	U.G.G.I., Ass.Met., Edinburgh, 1936, p. 66.
Sutcliffe, R.C.	1938	Quart.J.R. Met. Soc.,London, Vol. 64, p. 498.
	1947	Quart. J.R. Met. Soc., London, Vol. 73, p. 370.

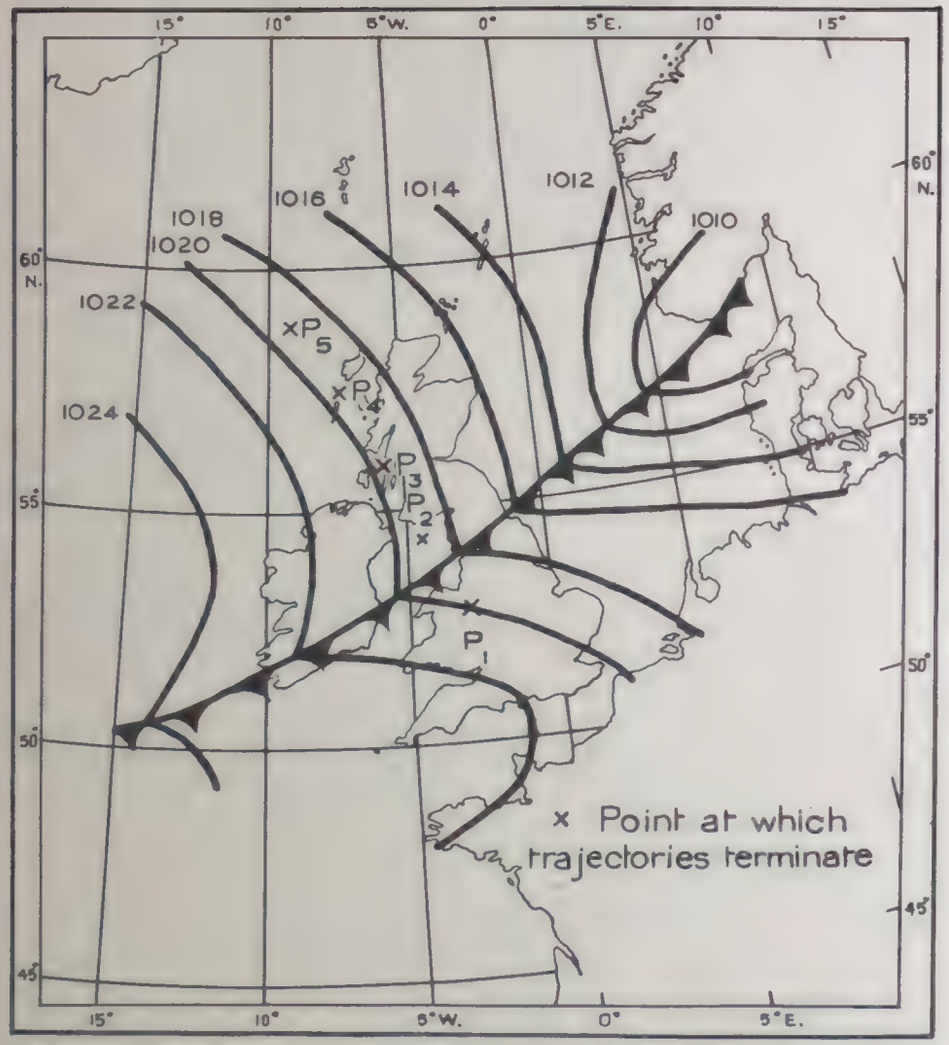

Fig. 1(a) Synoptic chart 0300 G.M.T., August 16, 1949.

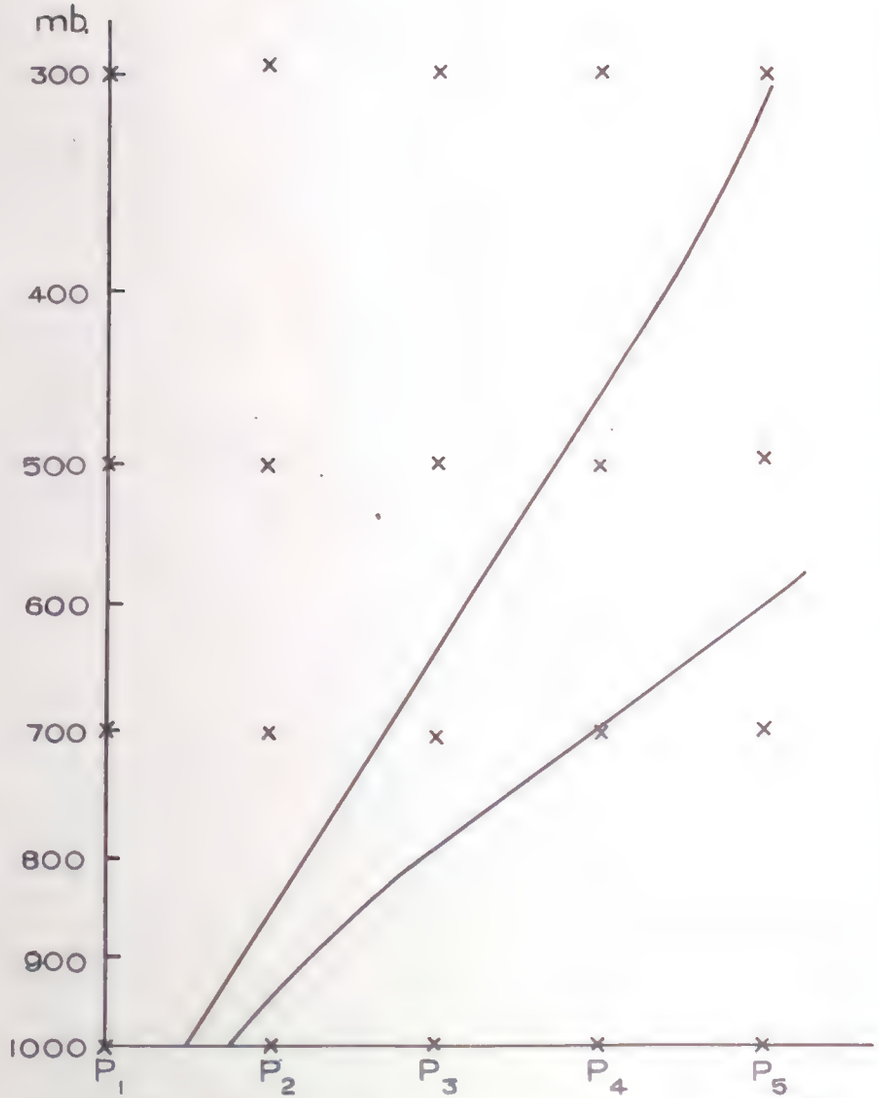

Fig. 1(b) Vertical cross-section for 0300 G.M.T., August 16, 1949, showing boundaries of frontal zone along the line on which trajectories terminate.

Fig.1. (c,d,e and f) 24 hour trajectories terminating in the frontal zone over the British Isles 0300 G.M.T. August 16 1949

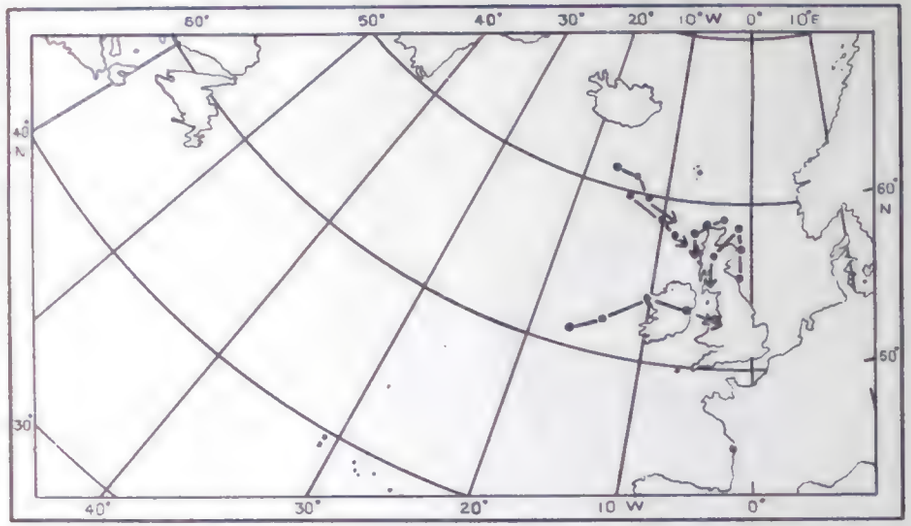

Fig.1 (c) Surface trajectories

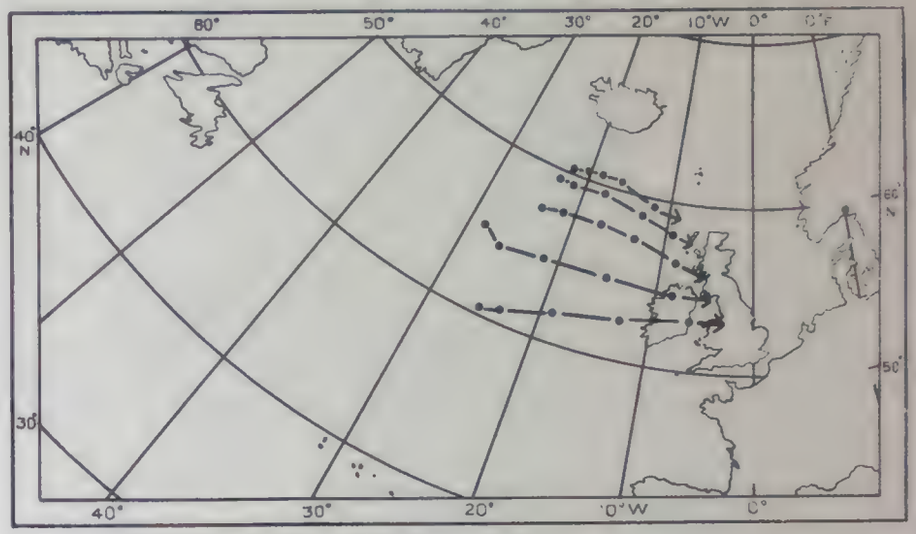

Fig.1(d) 700 mb. trajectories

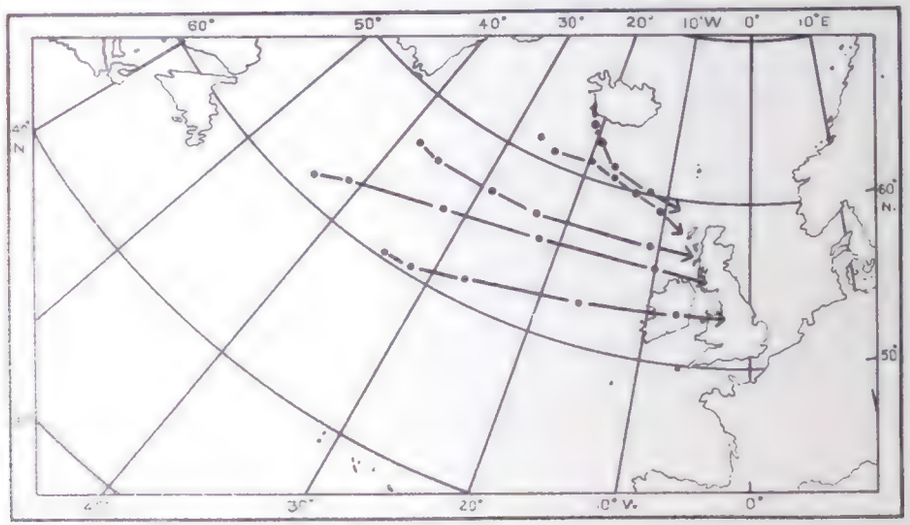

Fig.1(e) 500 mb. trajectories

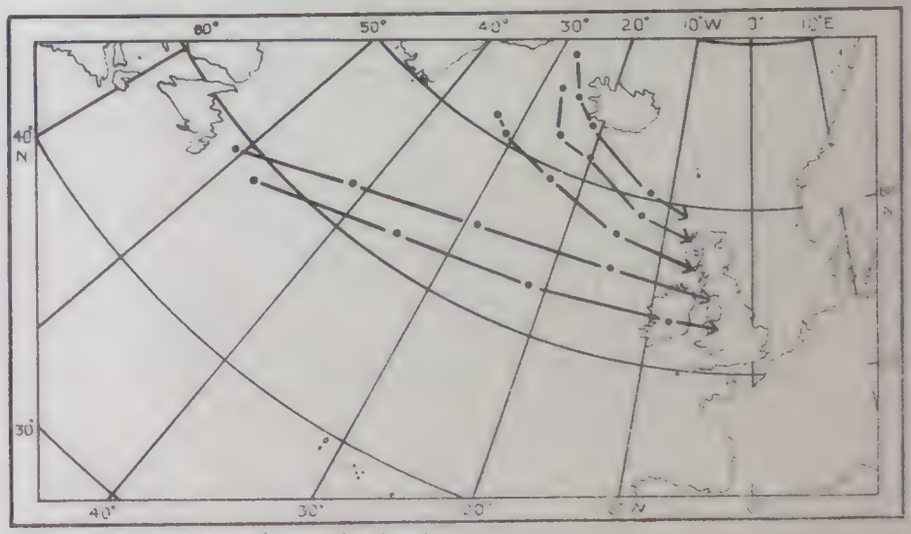

Fig.1(f) 300 mb. trajectories

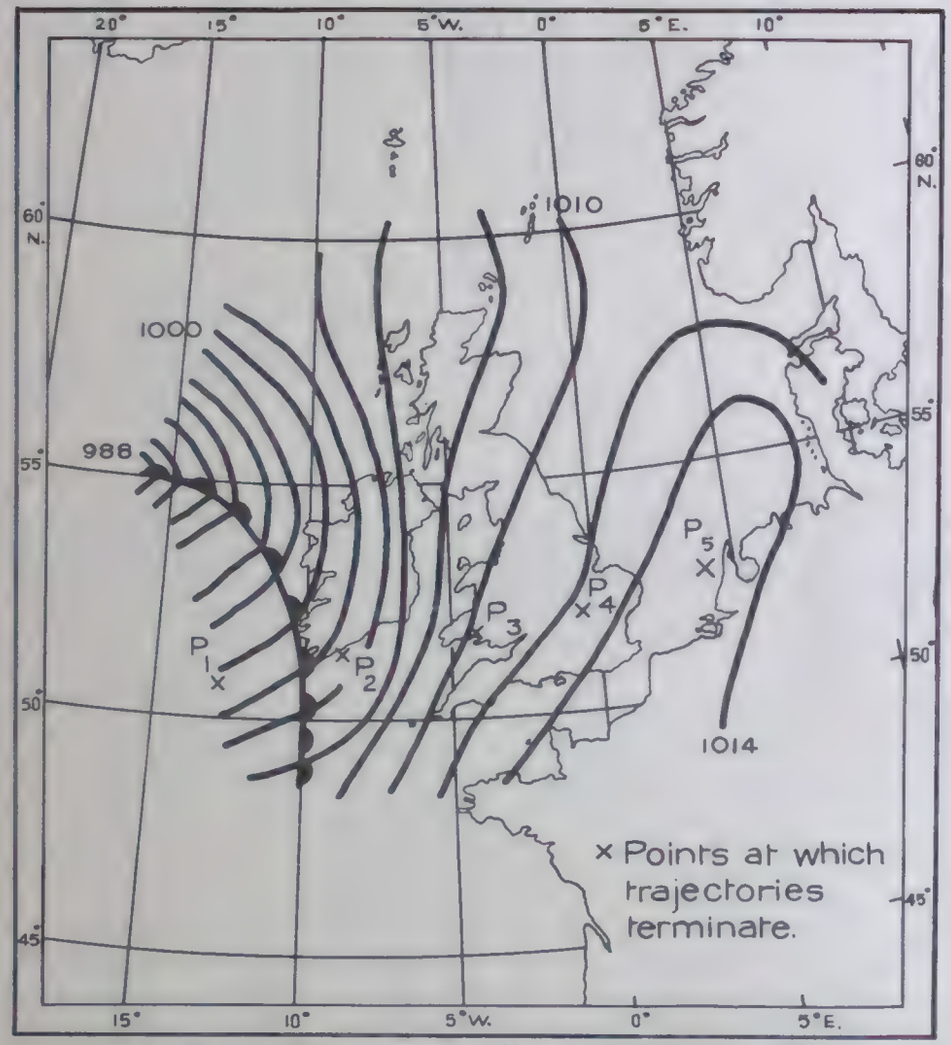

Fig. 2 (a) Synoptic chart 1500 G.M.T., May 3, 1948.

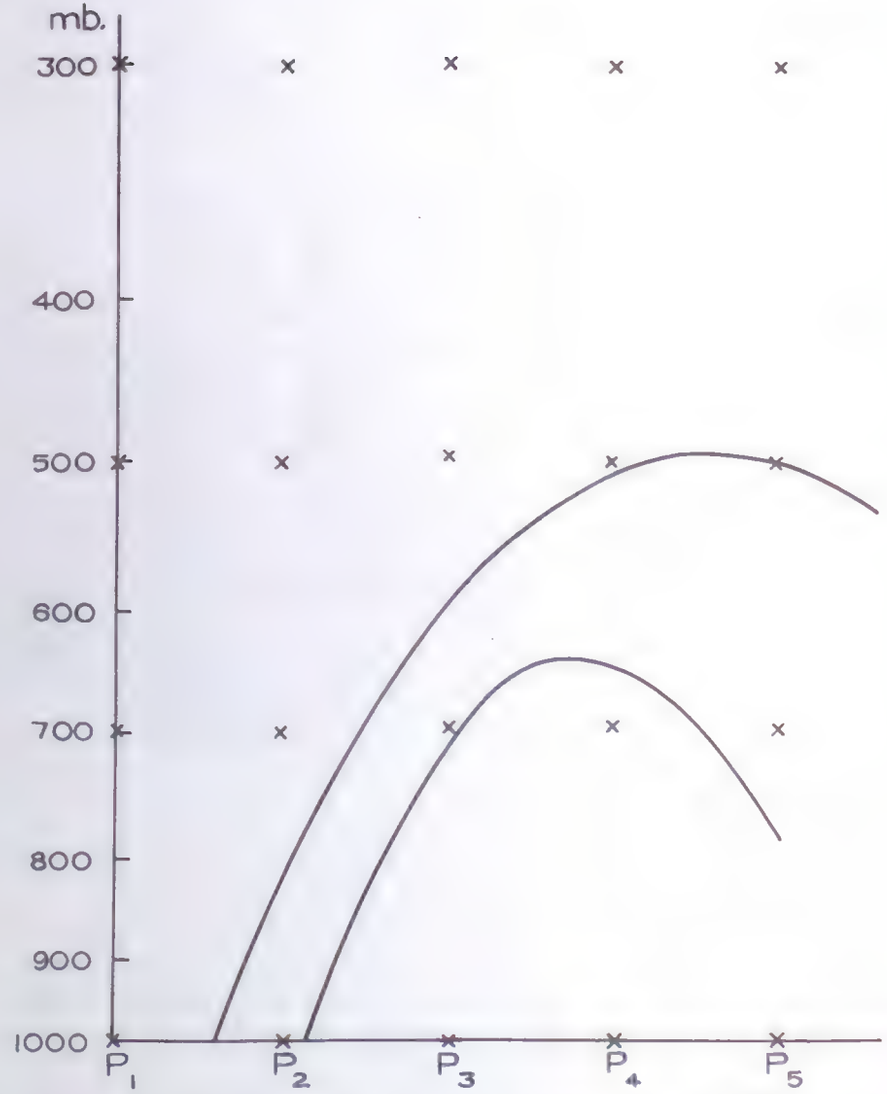

Fig.2 (b) Vertical cross-section for 1500 G.M.T., May 3, 1948, showing boundaries of frontal zone along the line on which trajectories terminate.

Fig.2 (c, d, e and F) 24 hour trajectories terminating in the frontal zone over the British Isles at 1500 G.M.T., May 3, 1948.

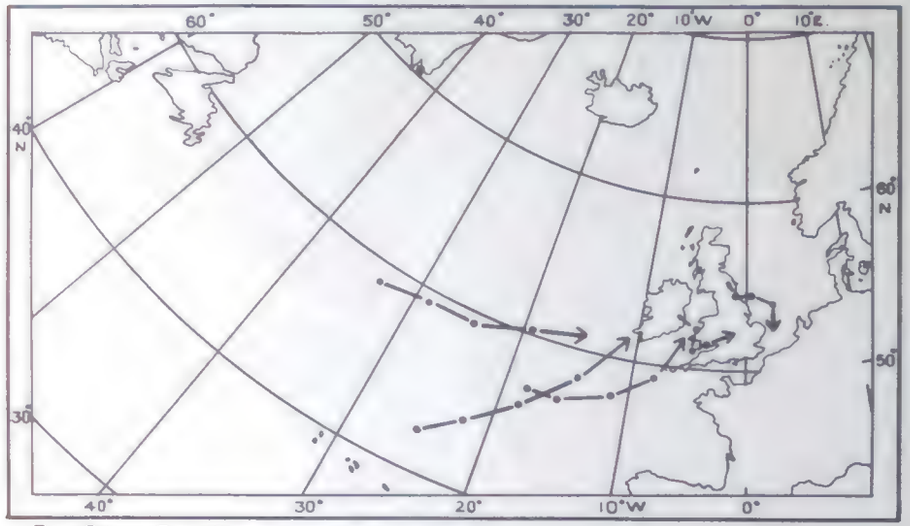

Fig.2(c) Surface trajectories

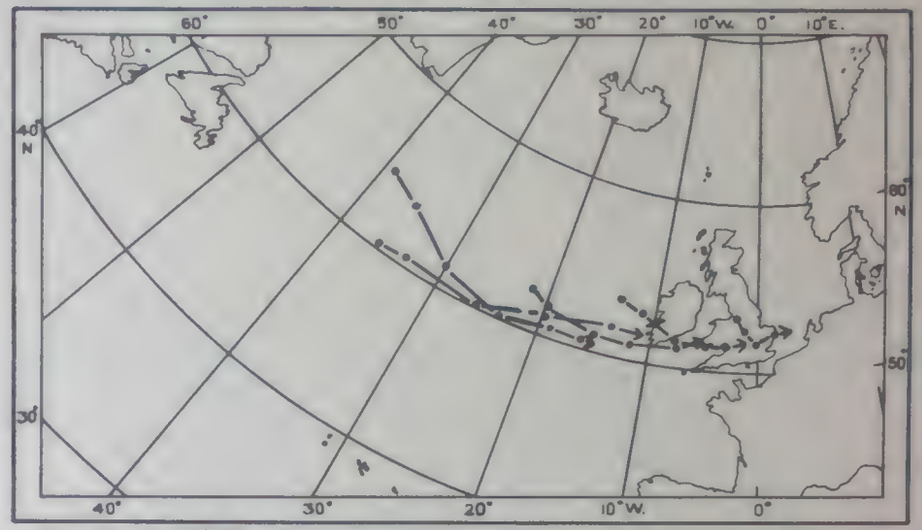

Fig. 2 (d) 700 mb. trajectories

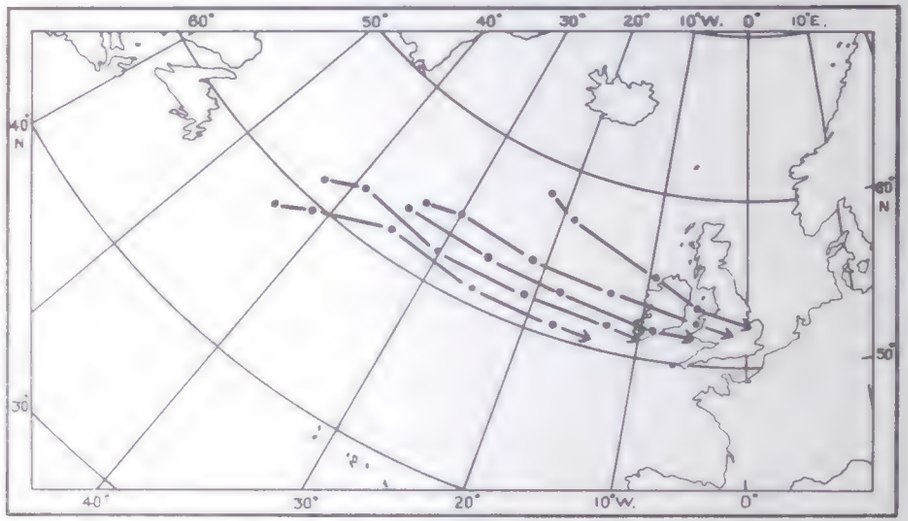

Fig.2(e) 500 mb. trajectories

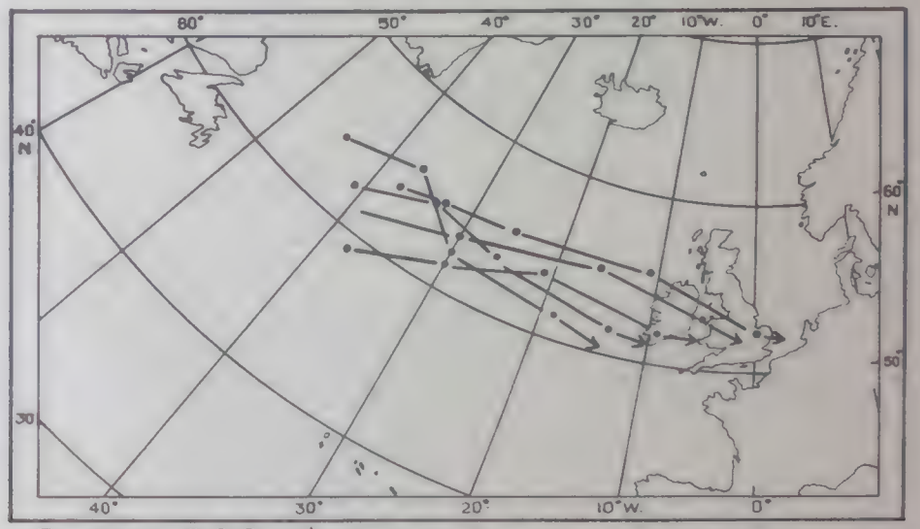

Fig. 2 (F) 300 mb. trajectories

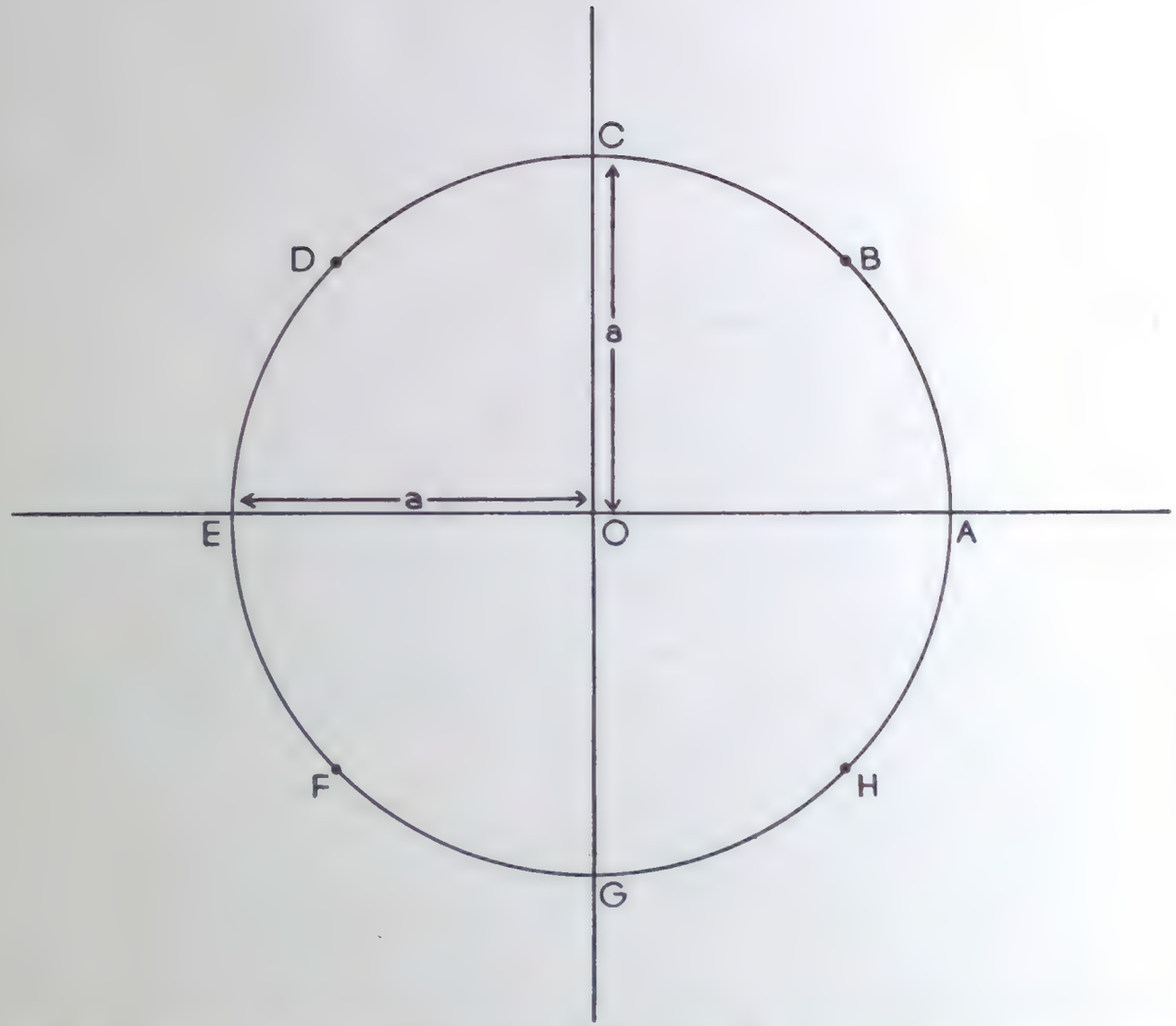

Fig. 3. Form of transparent scale used in estimating "Frontogenesis" from an isobaric chart.

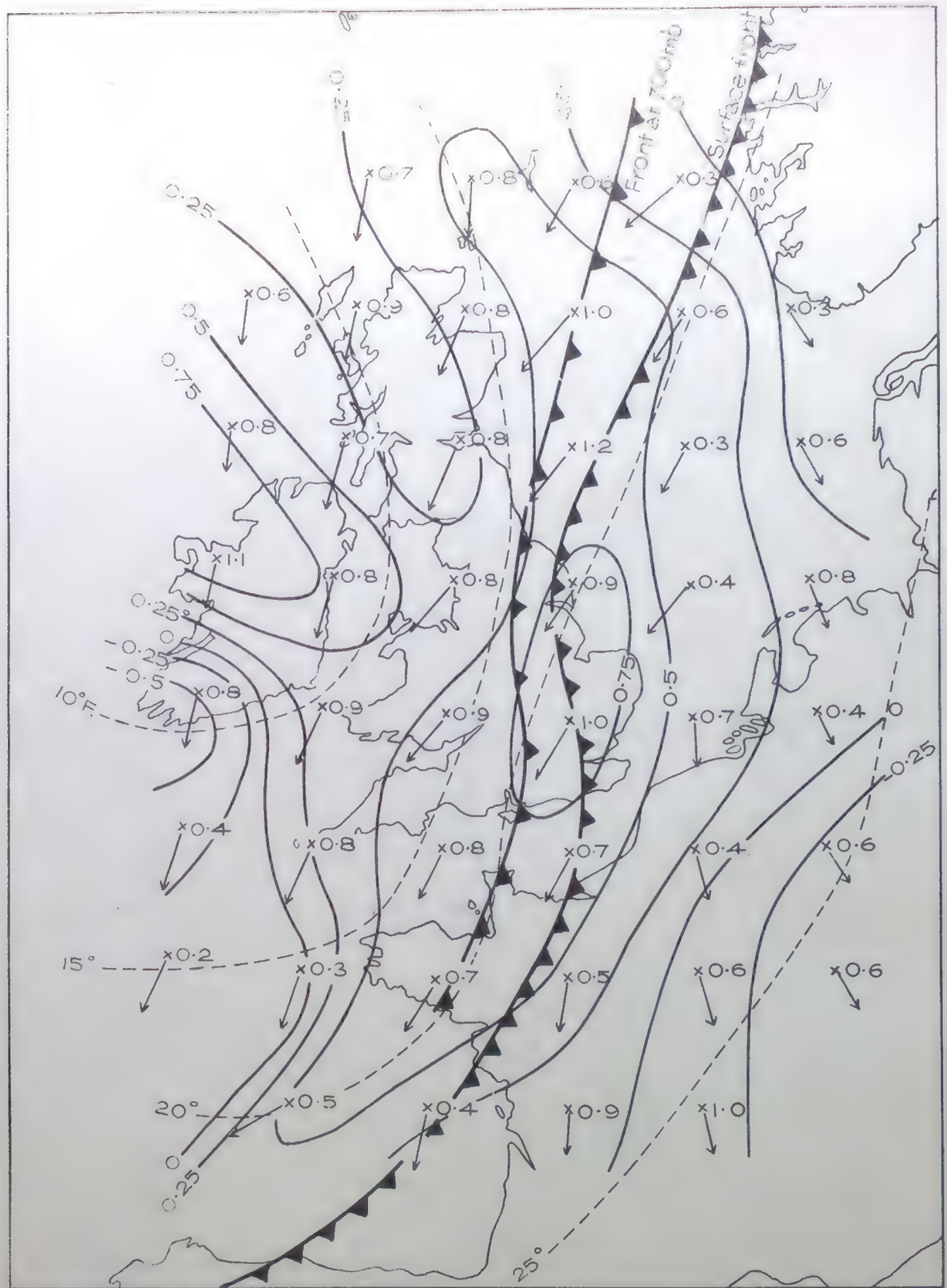

Fig. 4 Field of frontogenesis at 700 mb. 1800 G.M.T. November 5, 1949

———— Isopleths of $\frac{1}{2}(A^2+B^2)^{\frac{1}{2}} \cos 2\phi$

– – – – – Isotherms

Arrows indicate axis of dilatation and figures give value of $\frac{1}{2}(A^2+B^2)^{\frac{1}{2}}$ unit hr.$^{-1}$ ×10^{-1}

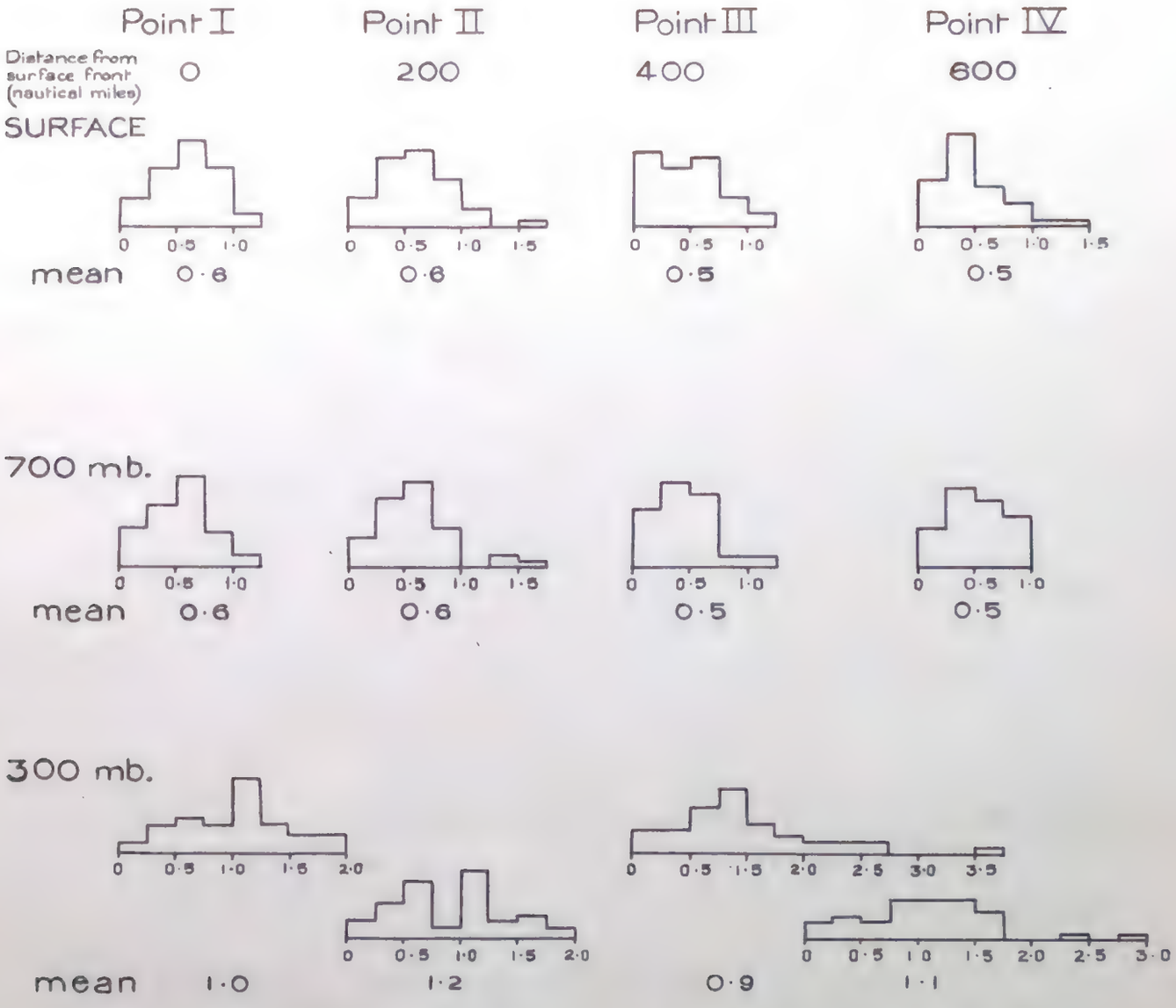

Fig.5 (a) Histograms showing the frequency of values of $\frac{1}{2}(A^2 + B^2)^{\frac{1}{2}}$ at points near active fronts (unit 10^{-1} hr^{-1})

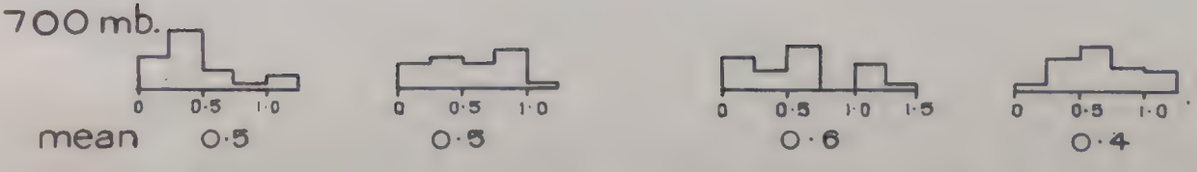

Fig.5(b) Histograms showing the frequency of values of $\frac{1}{2}(A^2 + B^2)^{\frac{1}{2}}$ at points near inactive fronts (unit 10^{-1} hr^{-1})

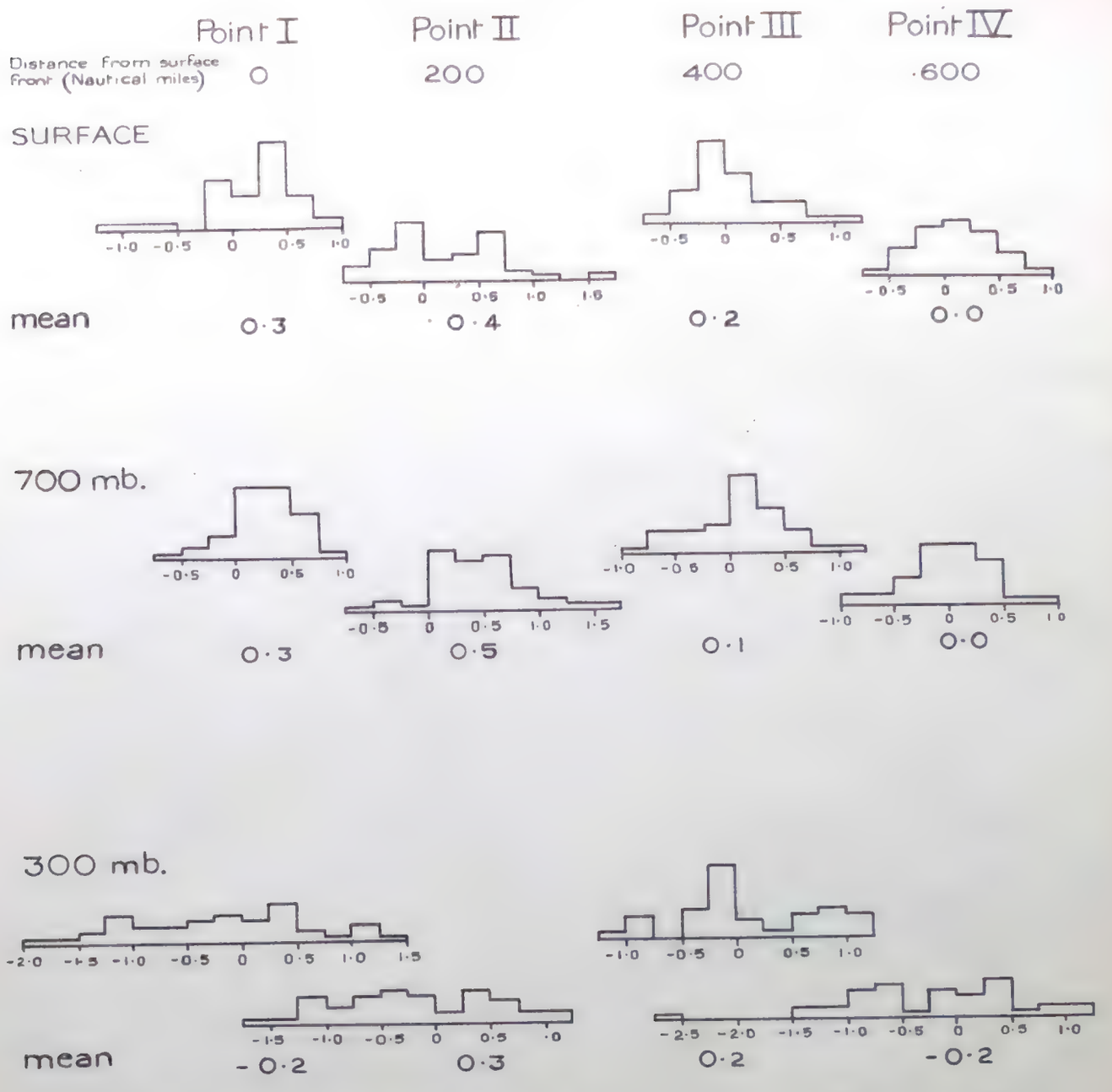

Fig.6(a) Histograms showing the frequency of values of $\frac{1}{2}(A^2 + B^2)^{\frac{1}{2}} \cos 2\phi$ at points near active fronts (unit $10^{-1}hr^{-1}$)

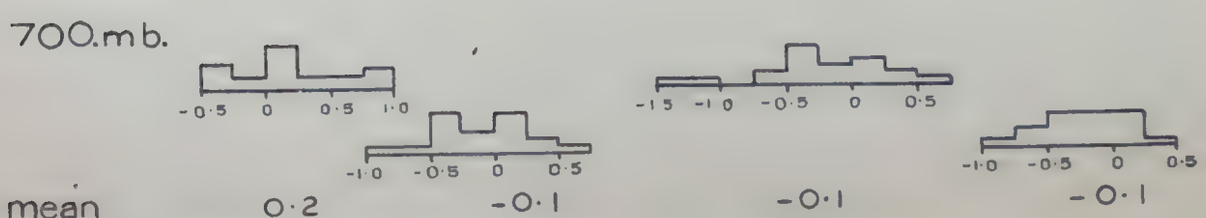

Fig.6(b) Histograms showing the frequency of values of $\frac{1}{2}(A^2 + B^2)^{\frac{1}{2}} \cos 2\phi$ at points near inactive fronts (unit $10^{-1}hr^{-1}$)

Fig. 7. Average field of frontogenesis in the vicinity of the warm front of January 16-17, 1951.
All values are averages over five charts from 0300 G.M.T. January 16 to 0300 G.M.T. January 17, 1951.

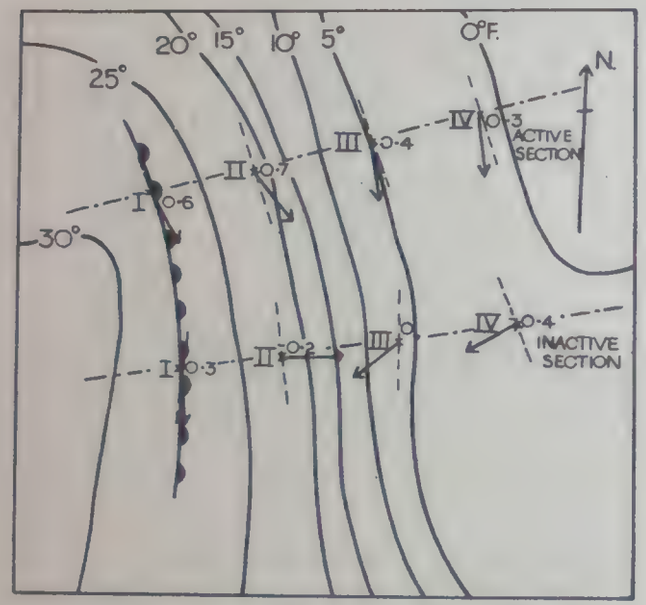

HORIZONTAL DISTRIBUTION OF TEMPERATURE AND FRONTOGENESIS AT 700 MB.

Arrows indicate axis of dilatation.

	I	II	III	IV
300mb.	0·8	0·3	1·0	0·8
500mb.	0·7	0·1	0·5	0·1
700mb.	0·6	0·7	0·4	0·3
1,000mb.	0·2	0·5	0·4	0·2

Active section of front.

	I	II	III	IV
300mb.	0·3	0·5	-0·1	-1·1
500mb.	0·5	0·3	0	-0·5
700mb.	0·3	-0·2	0	-0·4
1,000mb.	0·1	0·2	0·1	-0·1

Inactive section of front.

VERTICAL DISTRIBUTION OF FRONTOGENESIS

Numbers against each plotted point give values of $\frac{1}{2}(A^2+B^2)^{\frac{1}{2}} \cos 2\phi$ [Unit 10^{-1} hr.$^{-1}$]

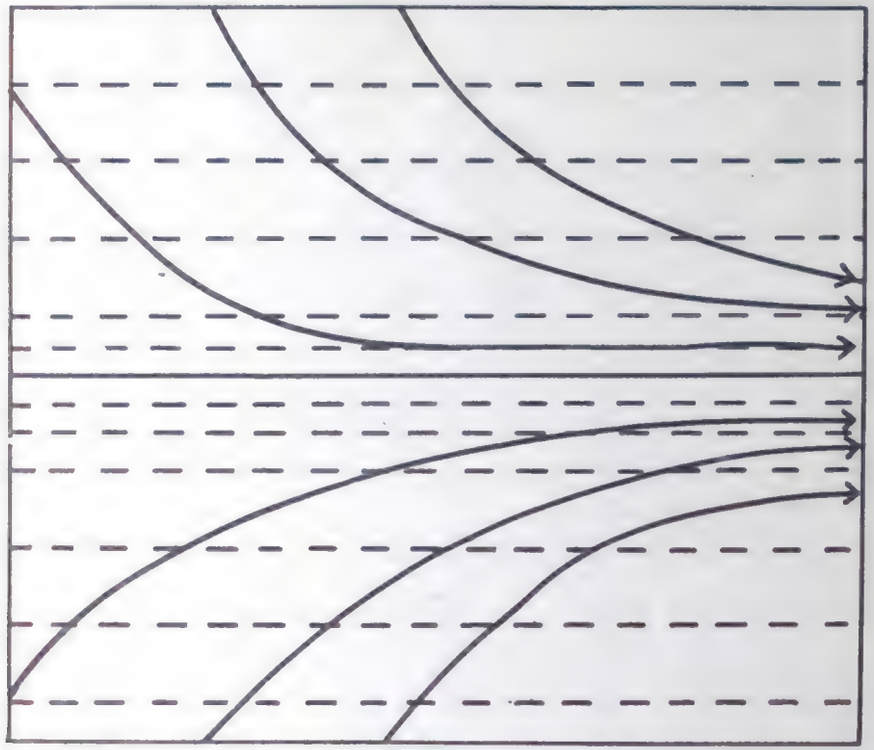

Fig 8a

Horizontal distribution of stream lines and isotherms in a frontogenetic confluence.

——— Stream lines

– – – Isotherms

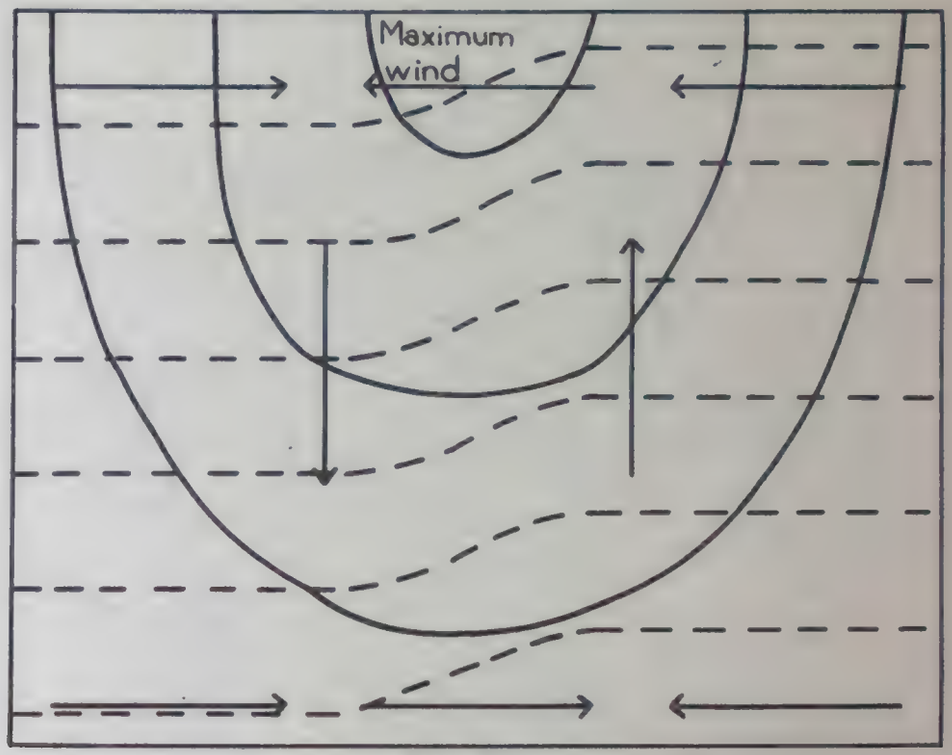

Fig 8b

Vertical section through frontogenetic confluence showing vertical circulation.

——— Isokinetics

– – – Isotherms

Fig. 9

CASE I — VERTICAL FRONTAL ZONE — DRY

Theoretical distribution of vertical and horizontal velocity and corresponding rate of change of specific volume

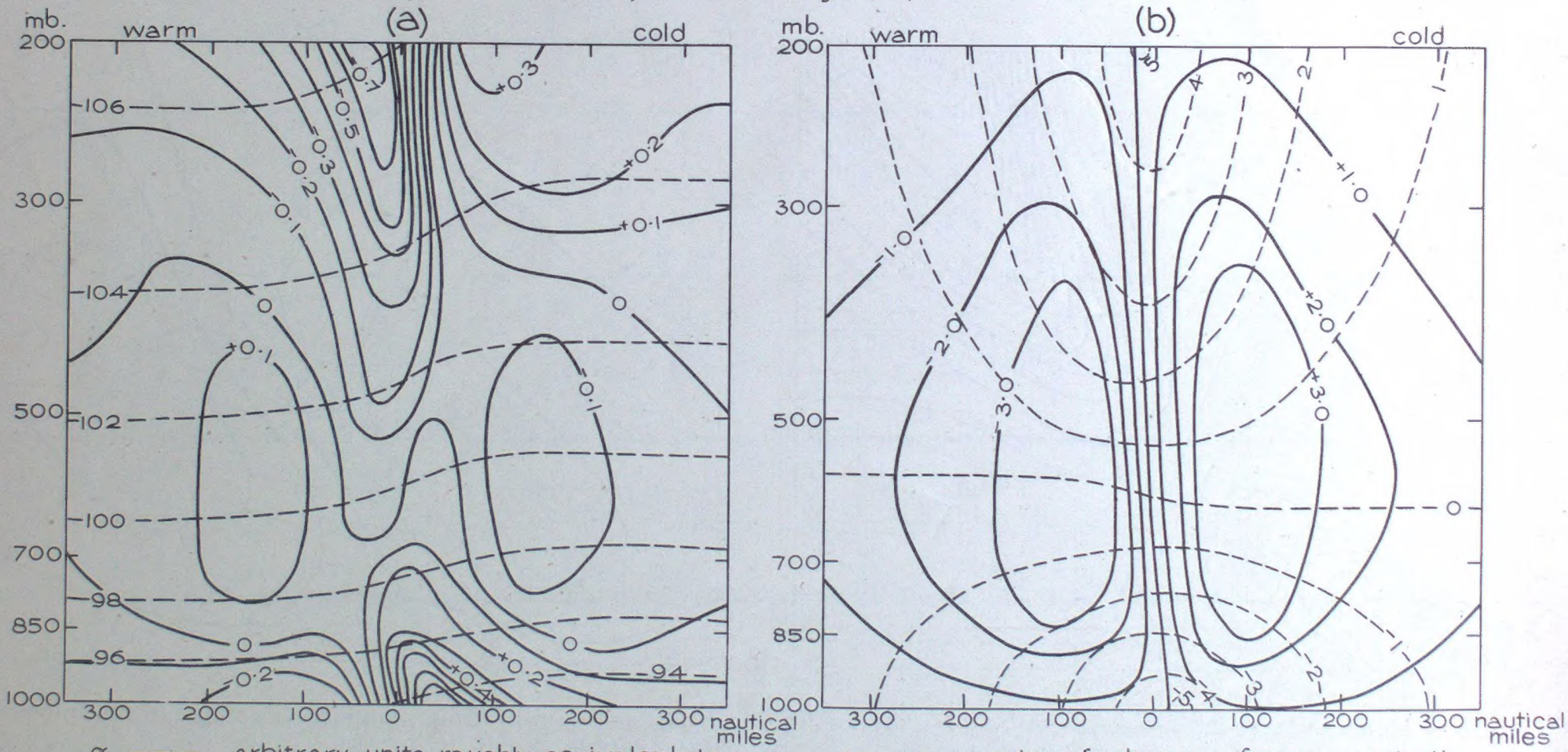

α ––– arbitrary units roughly equivalent to one hundredth of the specific volume at the ground in a standard atmosphere.

$\partial\alpha/\partial t$ ——— rate of change of α per hour

ω ——— rate of change of pressure in the moving air parcel i.e. dp/dt in mb./hr.

v_a ––– ageostrophic wind component in the y-direction in knots.

Fig. 10

CASE III — SLOPING FRONTAL ZONE — DRY

Theoretical distribution of vertical and horizontal velocity and corresponding rate of change of specific volume

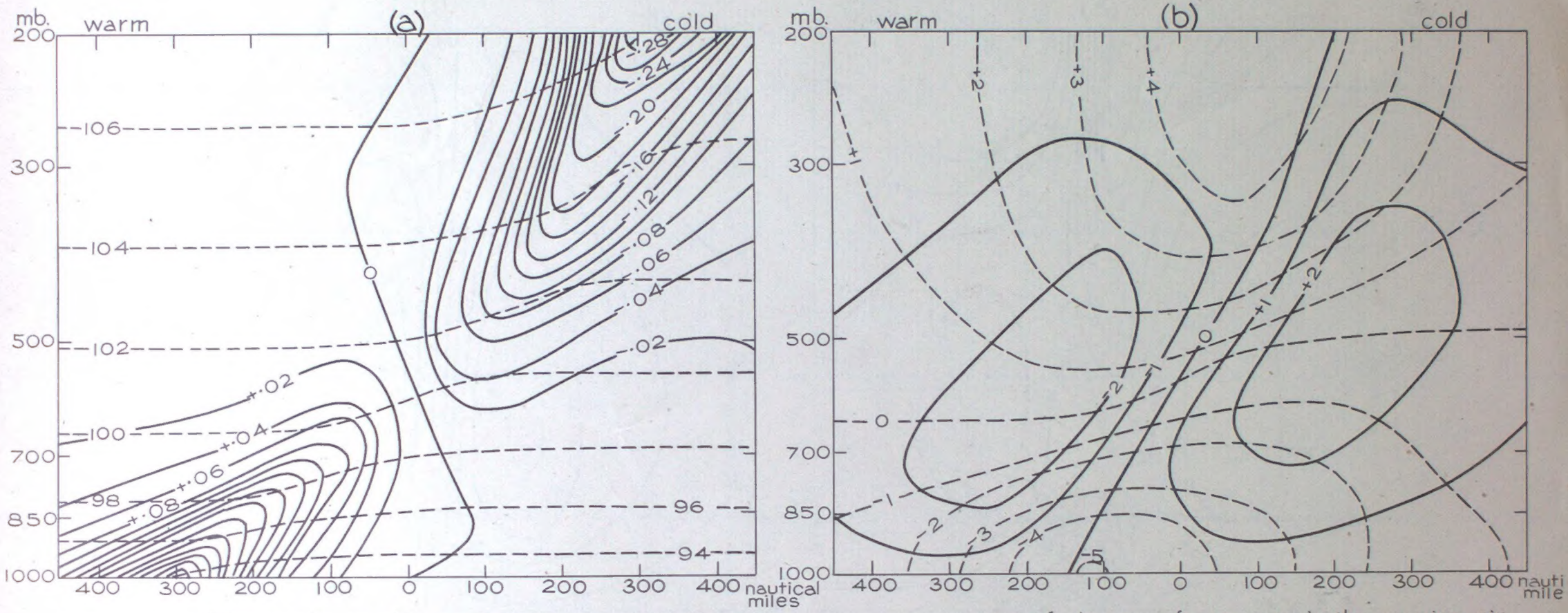

α ––– arbitrary units roughly equivalent to one hundredth of the specific volume at the ground in a standard atmosphere

$\partial\alpha/\partial t$ —— rate of change of α per hour

ω —— rate of change of pressure in the moving air parcel i.e. dp/dt in mb./hr.

v_a ––– ageostrophic wind component in the y-direction in knots

Fig.11 CASE IV — VERTICAL FRONTAL ZONE WITH VERTICAL CLOUDS

Theoretical distribution of vertical and horizontal velocity and corresponding rate of change of specific volume

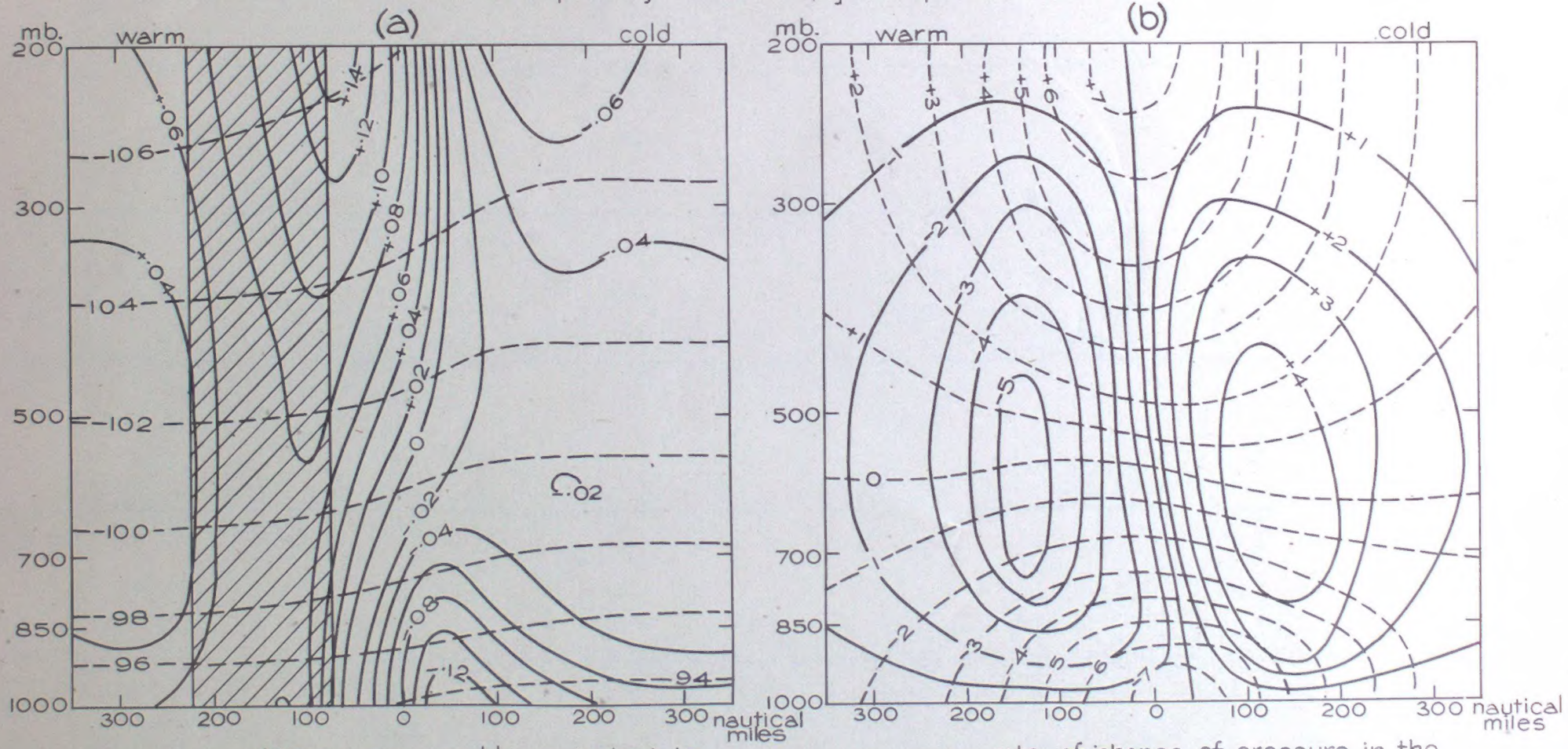

α ––– arbitrary units roughly equivalent to one hundredth of the specific volume at the ground in a standard atmosphere.

$\partial\alpha/\partial t$ ——— rate of change of α per hour

▨ area assumed to be occupied by cloud

ω ——— rate of change of pressure in the moving air parcel i.e. dp/dt in mb/hr.

v_a ––– ageostrophic wind component in the y-direction in knots

Fig. 12

CASE VI — SLOPING FRONTAL ZONE WITH CLOUD

Theoretical distribution of vertical and horizontal velocity and corresponding rate of change of specific volume

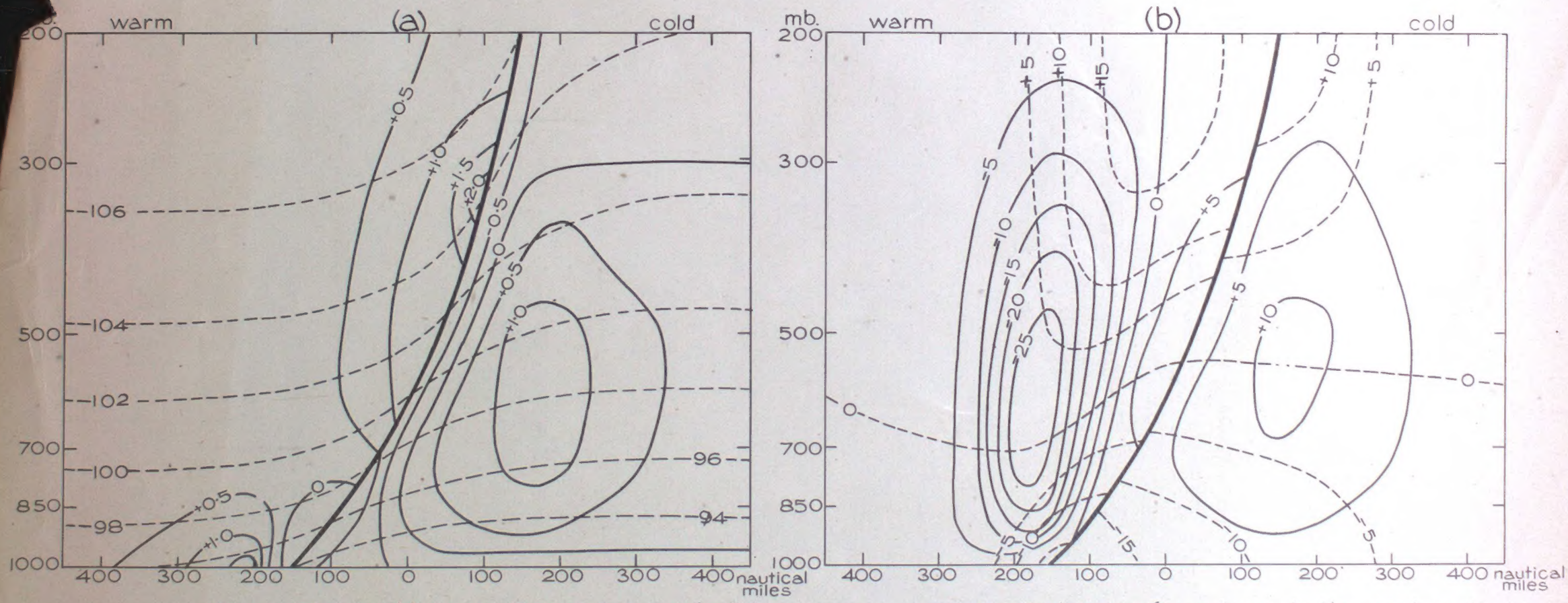

α --- arbitrary units roughly equivalent to one hundredth of the specific volume at the ground in a standard atmosphere

$\partial\alpha/\partial t$ —— rate of change of α per hour

ω —— rate of change of pressure in the moving air parcel i.e. dp/dt in mb/hr.

v_a --- ageostrophic wind component in the y-direction in knots

The area above and to the left of the thick sloping line is assumed to be saturated with water vapour; the remaining area is assumed dry